***Classification*:** Biological Sciences, Cell Biology

***Title*:** The collagen-binding proteoglycan fibromodulin can determine stroma matrix structure and fluid balance in experimental carcinoma

***Author affiliation*:** Åke Oldberg*, Sebastian Kalamajski*, Alexei V. Salnikov[†,‡,§], Linda Stuhr[¶], Matthias Mörgelin**, Rolf K. Reed[¶], Nils-Erik Heldin[††] and Kristofer Rubin[†]

*Department of Experimental Medical Sciences, BMC, B-12, University of Lund,
SE-221 84 Lund, SWEDEN
[†]Department of Medical Biochemistry and Microbiology, Uppsala University, BMC, Box 582
SE-751 23 Uppsala, SWEDEN
[‡]Oncology Clinic, University Hospital Lund, SE-221 85 Lund, SWEDEN
[¶]Department of Biomedicine, University of Bergen, N-5009 Bergen, NORWAY
[**]Department of Clinical Sciences, BMC B14, University of Lund, SE-221 84 Lund, SWEDEN
[††]Department of Genetics and Pathology, Uppsala University Hospital, Rudbeck Laboratory,
SE-751 85 Uppsala, SWEDEN

***Corresponding author*:** Kristofer Rubin Department of Medical Biochemistry and Microbiology, Uppsala University, BMC, Box 582 SE-751 23 Uppsala, SWEDEN Tel: +46 184714116,
Email: Kristofer.Rubin@imbim.uu.se

***Manuscript information*:** 13 text pages, 4 figures, and 2 tables.

***Word and character counts*:** 173 words in the abstract and 29846 characters in the paper

***Abbreviations footnote*:** Extra-cellular matrix (ECM). Interstitial fluid pressure (IFP). Soluble TGF-β receptor type II-murine Fc:IgG_{2A} chimeric protein (Fc:TβRII). Small leucine-rich repeat proteoglycan (SLRP). Human anaplastic thyroid carcinoma (KAT-4). Extra-cellular fluid volumes (ECV). Mus musculus fibromodulin gene (*Fmod*).

ABSTRACT

Research on the biology of the tumor stroma has the potential to lead to development of novel and more effective treatment regimes enhancing the efficacy of drug-based treatment of solid malignancies. Tumor stroma is characterized by distorted blood vessels and activated connective tissue cells producing a collagen-rich matrix. This is accompanied by elevated interstitial fluid pressure (IFP) indicating a transport barrier between tumor tissue and blood. Here we show that the collagen-binding proteoglycan fibromodulin controls stroma structure and fluid balance in experimental carcinoma. Gene ablation or inhibition of expression by anti-inflammatory agents showed that fibromodulin promoted the formation of a dense stroma and an elevated IFP. Fibromodulin-deficiency did not affect vasculature, but increased the extra-cellular fluid volume and lowered IFP. Our data suggest that fibromodulin controls carcinoma fluid balance by modulation of stroma matrix structure that in turn controls fluid convection inside and out of the stroma. This is particularly important in relation to the demonstration that targeted modulations of the fluid balance in carcinoma can increase the response to cancer therapeutic agents.

INTRODUCTION

In spite of advances in our knowledge of causative factors and genetic changes during development of the malignant genotype, treatment results and mean survival time for patients suffering from advanced cancer have improved only marginally. In recent years, partly in response to disillusion with the available cytotoxic cancer chemotherapeutic agents, attention has turned to the stromal elements of tumors. Abnormal blood vessels and connective tissue cells that produce a fibrotic collagen-rich matrix characterize the stroma of a carcinoma (1-4). Invasiveness and growth of malignant cells are affected by interactions with the stroma (5) and in this respect a carcinoma resembles an inflammatory lesion (6) or a wound that will not heal (7). A mathematical model of cancer invasion recently suggested that a heterogeneous extra-cellular matrix (ECM) with varying ECM component densities selects aggressive tumor cell phenotypes, whereas tumors with a homogenous ECM are less aggressive and invasive (8).

Carcinomas have a pathologically elevated interstitial fluid pressure (IFP) indicating a transport barrier between tumor tissue and blood (9-11). Indeed, pharmaceutical treatments that lower IFP in experimental carcinoma (12-14) and human cancers (15) also increase efficacy of cytostatic treatment. Treatment of mice carrying a xenografted human anaplastic thyroid carcinoma (KAT-4) with the soluble TGF-β receptor type II-murine Fc:IgG_{2A} chimeric protein (Fc:TβRII), which inhibits TGF-β1 and -β3, lowers IFP, reduces plasma protein leakage and enhances the anti-tumor effect of doxorubicin (16, 17). Microarray analyses (Affymetrix) of Fc:TβRII-treated KAT-4 carcinomas revealed down-regulations predominantly of macrophage-related genes (17). Furthermore, inhibition of IL-1 reduces IFP in these carcinomas (17). These findings indicate a role of inflammation in the generation of an elevated IFP. Tortuous and leaky blood vessels and absence of lymph drainage in tumors have also been suggested to be involved in the generation of the elevated tumor IFP. Inhibition of plasma protein leakage by interfering with vascular endothelial growth factor (VEGF) reduces IFP in experimental carcinomas (18, 19) and human colorectal adenocarcinoma (15). Little is known, however, about how the structure and composition of the ECM in the stroma influence carcinoma IFP.

The small leucine-rich repeat proteoglycan (SLRP) has a known role in collagen assembly and maintenance (20). Fibromodulin is expressed in dense regular connective tissues such as tendons, ligaments and cartilage, but is absent or expressed at low levels in skin, bone and visceral organs (21). Fibromodulin controls collagen matrix structure in tendons and ligaments and deficient mice show altered tissue organization with fewer and structurally abnormal collagen fiber bundles. The collagen fibrils are thinner (22), tendons and ligaments have reduced tensile strength and the animals develop knee-joint instability and osteoarthritis (23-25). Fibromodulin mRNA has been detected in a variety of clinical malignancies such as lung, breast and

prostate carcinomas (26-28). Here we report that fibromodulin has a role in regulating stroma ECM structure and fluid balance in carcinoma.

RESULTS

We were led to fibromodulin by the finding that in addition to lower expression of macrophage-related genes Fc:TβRII significantly down-regulated mRNA encoding fibromodulin. Notably, mRNA levels encoding other extracellular matrix (ECM) proteins such as collagen type I, fibronectin and the SLRP decorin were unchanged (Supplementary material). Initially we determined that fibromodulin showed a wide-ranging expression in experimental carcinomas such as chemically induced rat mammary carcinoma, mouse RIP-Tag insulinoma, transplantable syngeneic colonic carcinoma (PROb) and KAT-4 carcinoma growing as a xenograft in nude mice (Fig. 1). Staining was restricted to the stromal compartment in the carcinomas. This is consistent with the absence of fibromodulin in skin (21) and in cultured KAT-4 or PROb cells (data not shown). Quantitative PCR analyses showed that treatment of KAT-4 carcinomas with Fc:TβRII reduced fibromodulin mRNA by approximately 50% (Fig. 1D). Immunohistochemical analyses showed that fibromodulin protein expression was also reduced (Figs. 1E-F). No staining was seen in carcinomas from fibromodulin-deficient mice (Fig. 1H).

Fibromodulin-deficient nu/nu mice were used further to study the role of fibromodulin in tumors. Human KAT-4 carcinoma cells were transplanted subcutaneously in wild type, *Fmod*-null and heterozygous nu/nu littermates. Tumor take, length of lag phase and temporal increase in external sizes were identical in the three genotypes. Total carcinoma weights 31 days after transplantation averaged 0.54 ± 0.26 g (average ± SD, $n = 8$) in wild type, and 0.54 ± 0.21 g ($n = 6$) in fibromodulin-deficient mice. DNA content averaged 5.8 mg DNA/g wet weight ± 0.6 (± SD, $n = 5$) in wild type, and 5.8 ± 0.3 ($n = 7$) in fibromodulin-deficient mice indicating that fibromodulin had no influence on tumor cellularity.

Stromal collagen fibrils in wild type and heterozygous mice were similar with an average diameter of 43 nm, while those grown in fibromodulin-deficient mice were significantly thinner (30 nm) (Fig. 2 A, B and E). The gross structures of the collagen scaffold also differed, with thicker and more abundant collagen fiber bundles in wild type stroma (Fig. 2 G-H). Analyses of whole-mount carcinomas showed that the density of the collagen scaffold was 25% ($p < 0.008$) higher in wild type (60 ± 4 pixels / area unit, $n = 4$) compared to fibromodulin-deficient carcinomas (45 ± 0.5 pixels / area unit, $n = 4$). A similar dependence on fibromodulin for collagen scaffold structure was also observed in PROb rat colorectal adenocarcinoma (data not shown). Fc:TβRII treatment, which reduces fibromodulin, resulted in similar collagen fibril diameters and scaffold

structures as in the stroma of KAT-4 carcinomas grown in fibromodulin-deficient mice (Fig. 2 C, D and F). Two discrete populations arose after treatment with Fc:TβRII, characterized by thin fibrils similar to those in *Fmod*-null stroma and wider fibrils, presumably formed prior to treatment. The collagen scaffold gross structure after Fc:TβRII treatment and in fibromodulin-deficient stroma were similar (Fig. 2 J, H). Fc:TβRII treatment reduced collagen density by 21% ($p \leq 0.03$). Collagen densities in control carcinomas (IgG_{2A}-treated) were 62 ± 4 pixels/unit area ($n = 3$) compared to 49 ± 3 pixels/unit area ($n = 3$) in Fc:TβRII treated carcinomas. These results are consistent with our previous observation of a 35% reduction in hydroxyproline after Fc:TβRII treatment of KAT-4 carcinomas (16) and suggest a role for fibromodulin in the assembly of the collagen scaffold.

IFP was lower in KAT-4 and PROb experimental carcinomas grown in fibromodulin-deficient mice (Fig. 3). Average IFP values were 5.7 ± 2.0 mm Hg (± SD, $n = 10$) in wild-type, 4.7 ± 1.2 mm Hg ($n = 9$) in heterozygous and 3.7 ± 1.3 mm Hg ($n = 15$, $p < 0.05$) in fibromodulin-deficient KAT-4 carcinomas. PROb carcinomas showed IFP values of 5.6 ± 1.7 mm Hg (n = 4) when grown in wild-type mice, 4.3 ± 1.6 mm Hg in *Fmod* +/- ($n = 4$) and 2.6 ± 1.8 mm Hg in *Fmod* -/- ($n = 5$). The differences between wild-type and fibromodulin-deficient mice were significant ($p < 0.05$) assuming a Gaussian distribution of the values. IFP averages in tumors grown in heterozygous mice were intermediate but not significantly different from IFP averages recorded in any of the other genotypes, indicating a dose dependent effect of fibromodulin.

Fibromodulin-deficiency had no apparent effect on the vasculature since densities of CD31-expressing endothelial structures (Fig. 4A), plasma protein leakage and perfused vessels were not significantly different in KAT-4 carcinomas grown in wild-type or fibromodulin-deficient mice (Table I). Furthermore, plasma volumes in KAT-4 carcinomas were unaffected (Table II). KAT-4 carcinomas grown in fibromodulin-deficient mice had, however, significantly increased extra-cellular fluid volumes (ECV) (Table II). The ECV in the skin of the two genotypes were similar (Table II).

Fibromodulin deficiency had no effect on the number of macrophages or their expression of MHC class II in KAT-4 tumor viable tissue (Figs. 4B and C). Anti-inflammatory agents, such as dexamethasone and recombinant human IL-1 receptor antagonist (rh-IL-1Ra), efficiently down-regulated the expression of fibromodulin mRNA and immunoreactive fibromodulin in KAT-4 carcinomas (Fig. 4D and data not shown).

DISCUSSION

Here we show that fibromodulin promotes the formation of a dense collagen scaffold in experimental carcinoma. Absence or reduction of fibromodulin resulted in a lowering of IFP. The data indicate that

fibromodulin deficiency resulted in increased compliance and/or hydraulic conductivity of the stroma leading to an increased ECV. Furthermore, we did not detect any vascular differences between wild-type and fibromodulin-deficient KAT-4 carcinoma. This strongly suggests that factors beyond the vasculature are responsible for the reduction in IFP and increase in ECV in fibromodulin-deficient KAT-4 carcinoma. Our results indicate that the changes in fluid balance are caused by alterations in stroma collagen content and architecture.

The tumor stroma is generated by carcinoma cell-driven activation of normal, *i.e.* non-transformed host cells, such as endothelial cells, pericytes and fibroblasts. Carcinoma cells may activate such stroma target cells directly and/or indirectly via infiltrated immune cells. In recent years much focus has been directed to the role of macrophages for the development of a tumor stroma. Activated macrophages in carcinoma modulate their microenvironment (6), and are conversely modulated by a hypoxic microenvironment (29). Our data show that fibromodulin does not affect macrophage numbers or their expression of MHC class II antigens, the latter reportedly reflecting macrophage activation (30). Treatment of KAT-4 carcinomas with Fc:TβRII reduces inflammatory characteristics (17) and down-regulated fibromodulin expression (present findings). In agreement, the anti-inflammatory agents dexamethasone and IL-1 receptor antagonist down-regulated fibromodulin expression. The same agents and Fc:TβRII reduce IFP in KAT-4 carcinomas (16, 17) (and unpublished). Dexamethasone reduces IFP also in other types of experimental carcinomas (31). Thus our findings suggest that inflammatory processes in carcinomas promote fibromodulin synthesis by stroma cells, leading to the formation of a dense and stiff collagen scaffold and a high IFP.

Desmoplasia is a feature of most carcinomas but the potential use of staging the desmoplasia as a prognostic marker remains controversial (32, 33). It is likely that, in addition to the amount of stroma, the architecture and functional properties of the collagen scaffold correlates with malignancy (8). In carcinomas, resembling wounds, collagen turnover is generally high (34). Fibromodulin and other SLRPs bind and protect collagen fibrils from degradation by collagenases *in vitro* (35). Recent studies in our laboratories suggest that collagen turnover in tendons is increased in fibromodulin-deficient mice indicating a protective role for fibromodulin against degradation also *in vivo* (SK, ÅO, unpublished observation). Alternatively, fibromodulin may affect the collagen fibril assembly by binding and aligning monomeric triple helical collagen and thin fibrils in the growing fibril. A proper alignment of collagen is essential for interactions and the formation of cross-links in the growing fibril. An increased turnover may in part be due to misaligned collagen fibrils that are rapidly degraded in fibromodulin-deficient tendons. The present findings of fibromodulin-directed regulation of collagen assembly in carcinoma suggests that fibromodulin synthesis constitutes a mechanism providing a stable collagen scaffold that otherwise would be rapidly degraded.

It has been demonstrated that the ECM composition determines hydraulic conductivity in tissues (36). Furthermore, irradiation of experimental tumor increases collagen content but reduces hydraulic conductivity (37). The reduced amount of collagen in fibromodulin-deficient carcinoma would by itself raise the hydraulic conductivity. The increased ECV will also contribute to increased conductivity in the stroma by effectively diluting matrix components (36). The increased hydraulic conductivity will favor a flow of fluid from parts of the tumor with a high IFP to the periphery where IFP is lower. Such a redistribution of fluid should result in a general reduction of IFP in the carcinoma as seen in fibromodulin-deficient KAT-4 carcinomas. The increased ECV in fibromodulin-deficient carcinomas also suggests that the collagen scaffold is less stiff, allowing tumors to swell due to the high plasma protein content in the carcinoma interstitium that results from the leaky blood vessels. Indeed, treatment of fibromodulin-deficient KAT-4 carcinomas with Fc:TβRII that decreases plasma protein leakage (17) reduced the ECV. An increased hydraulic conductivity and fluid flow in carcinomas may also explain the increased efficacy of chemotherapy in KAT-4 carcinomas pretreated with Fc:TβRII (17). Several agents reduce IFP and some increase the delivery and efficacy of chemotherapeutics (11). Here we show that one of these agents, Fc:TβRII reduces fibromodulin expression. Furthermore, the collagen scaffold restricts diffusive transport of macromolecules in the stroma of experimental carcinoma (10, 38) and thus most likely the delivery of high-molecular weight anti-cancer drugs. The unexpected role for fibromodulin in controlling carcinoma fluid balance may provide a basis for a novel treatment to improve delivery of anti-cancer drugs by modulation of fibromodulin expression.

METHODS

Animals and tumors

Fibromodulin-deficient mice were generated and maintained in 129/SV background (22). *Fmod*-null mice were crossed with C57Bl nu/nu mice to generate male (nu/nu, *Fmod* +/-) and female (nu/nu +/-, *Fmod* +/-). All experiments were conducted on nu/nu littermates generated by breeding male (nu/nu, *Fmod* +/-) and female (nu/nu +/-, *Fmod* +/-). Mice were genotyped as described (25). KAT-4 anaplastic thyroid carcinoma cells (5 x 10^6) or rat PROb (5 x 10^6) colonic carcinoma cells were injected *s.c.* in the left flank of the mice and treatment with Fc:TβRII (10 mg/kg) was performed as described (14, 16). All animal experiments were approved by the Ethical Committee for Animal Experiments in Uppsala and in Lund (Sweden). The number of animals was minimized to comply with guidelines from the Ethical Committee.

In vivo perfusion and permeability assay.

Perfused tumor vessels were visualized using FITC-dextran (molecular weight 2,000 kDa) (Sigma, St. Louis, MO). Vascular permeability was assessed by determining leakage of Evans Blue dye (EBD) into the tumor tissue interstitium. 30 mg/kg EBD (Sigma, St. Louis, MO) was administered *i.v.* 30 minutes and FITC-Dextran (100 mg/kg) two minutes prior to animal sacrifice. To evaluate the perfused area of tumor vasculature

and leakage of EBD, 20 μm frozen sections were analyzed by fluorescent microscopy. Images were obtained from 16 fields of vision from 8 sections per tumor taken 100 μm apart and assessed under low magnification. Images were analyzed using a Nikon Labophot microscope and captured with a SPOT Insight digital camera (Diagnostic Instruments, Sterling Heights, MI), using the SPOT 3.4 software. The extent of EBD leakage was analyzed using NIH Image 1.62 software from the National Institute of Health (Bethesda, MD, USA). Digital images were analyzed in a gray-scale mode and dye density in tumor sections was presented as number of pixels per area of tumor tissue. The density of FITCdextran-perfused vessels was quantified in 16 fields of vision with high vascular density under low magnification according to Chalkley point-overlap morphometry. Using this method, the mean of perfused vessel densities of the most vascular areas within the tumor (*x* 200 magnification) are calculated manually. Selected areas ('hot spots') were identified after scanning the whole section at low magnification. This technique has been established as a standard method for quantification of angiogenesis in sections from solid tumors.

Quantitative real time PCR

Total RNA was extracted from KAT-4 tumors using RNAeasy kit (Qiagen) and TRIZOL solution (Invitrogen, San Diego, CA), DNase I treatmented and a first-strand cDNA synthesis was performed (first-strand synthesis kits from Roche Diagnostics, Penzberg, Germany, or iScript from Bio-Rad Laboratories, Sundbyberg, Sweden) using oligo-dT primers. The cDNA samples were mixed with specific primers and SYBR Green and amplified in a ABI Prism instrument (Applied Biosystem, Foster City, CA) starting with an initial 10 min heating at 95°C followed by 40 cycles at 95°C for 15 s, 60°C for 30 s, and 72°C for 30 s. The data were analyzed using SDS 2.1 software (Applied Biosystems). The calculated threshold cycle (Ct) values were normalized to the Ct-value for β-actin or glyceraldehyde-3-phosphate dehydrogenase (GAPDH) used as internal standard. The primers used were: Fmod: 5'- AGCAGTCCACCTACTACGACC-3' and 5'-CAGTCGCATTCTTGGGGACA-3', β-actin: 5'- GGCACCCAGCACAATGAAG-3' and 5'-GCCGATCCACACGGAGTACT-3', GAPDH: 5'-AGGTCGGTGTGAACGGATTTG-3' and 5'-TGTAGACCATGTAGTTGAGGTCA-3'

Electron microscopy

Three similarly sized tumors from wild type, fibromodulin deficient, IgG_{2A}-treated, and Fc:TβRII-treated mice were investigated by transmission electron microscopy. Carcinomas were fixed in 0.15 M sodium cacodylate-buffered 2% glutaraldehyde, postfixed in 0.1 M *s*-collidine-buffered 2% osmium tetroxide and embedded in epoxy resin (22). Ultrathin sections were analyzed in Philips CM-10 electron microscope. Scanning electron microscopy was performed on whole-mount specimens prepared by alkali maceration (39) and analyzed in PHILIPS 515 electron microscope. For quantification of matrix amount, the images were converted to white and black pixels that represented matrix and empty areas, respectively. Pixels were quantified with ImageJ software (NIH, USA) in three whole mount carcinomas of similar size from control and Fc:TβRII-treated carcinomas, and from carcinomas grown in wild type and fibromodulin-deficient mice. Collagen densities are expressed as percent of area occupied by matrix.

Statistical methods

The unpaired, two-tailed Student's *t*-test was used. The Mann-Whitney *U* test was used when data failed to fulfill the normality criteria. $p < 0.05$ was considered statistically significant. Standard deviations of means are indicated in the figures unless otherwise specified.

FOOTNOTES

[§]Present address: Division of Molecular Immunology, German Cancer Research Center, Heidelberg, Germany

ACKNOWLEDGEMENTS
We thank Ms Ann-Marie Gustafson, Annika Hermansson and Gerd Salvesen for technical assistance. This study was supported by grants from the Swedish Cancer Foundation (KR, NEH), Swedish Research Council (NEH, ÅO, KR), Gustaf V:s 80-Anniversary Fund (KR, ÅO), Greta and Johan Kocks and Alfred Österlunds Funds (ÅO), Gunnar Nilssons Cancer Organization (KR) and the Norwegian Research Council (RKR and LS).

REFERENCES

1. Hashizume, H, Baluk, P, Morikawa, S, McLean, JW, Thurston, G, Roberge, S, Jain, RK & McDonald, D M (2000) *Am J Pathol* 156: 1363-80.
2. Mueller, MM & Fusenig, NE (2004) *Nat Rev Cancer* 4: 839-49.
3. Bhowmick, NA, Neilson, EG & Moses, HL (2004) *Nature* 432: 332-7.
4. Liotta, LA & Kohn, EC (2001) *Nature* 411: 375-9.
5. Hanahan, D & Weinberg, RA (2000) *Cell* 100: 57-70.
6. Coussens, LM & Werb, Z (2002) *Nature* 420: 860-7.
7. Dvorak, HF (1986) *N Engl J Med* 315: 1650-9.
8. Anderson, AR, Weaver, AM, Cummings, PT & Quaranta, V (2006) *Cell* 127: 905-915.
9 Jain, RK (1987) *Cancer Res* 47: 3039-51.
10 Netti, PA, Berk, DA, Swartz, MA, Grodzinsky, AJ & Jain, RK (2000) *Cancer Res* 60: 2497-503.
11. Heldin, C-H, Rubin, K, Pietras, K & Ostman, A (2004) *Nat Rev Cancer* 4: 806-13.
12. Emerich, DF, Dean, RL, Snodgrass, P, Lafreniere, D, Agostino, M, Wiens, T, Xiong, H, Hasler, B, Marsh, J, Pink, M, Kim, BS, Perdomo, B & Bartus, RT (2001) *J Pharmacol Exp Ther* 296: 632-41.
13. Pietras, K, Rubin, K, Sjoblom, T, Buchdunger, E, Sjoquist, M, Heldin, C-H & Ostman, A (2002) *Cancer Res* 62: 5476-84.
14. Salnikov, AV, Iversen, VV, Koisti, M, Sundberg, C, Johansson, L, Stuhr, LB, Sjoquist, M, Ahlstrom, H, Reed, RK & Rubin, K (2003) *Faseb J* 17: 1756-8.
15 Willett, CG, Boucher, Y, Di Tomaso, E, Duda, DG, Munn, LL, Tong, RT, Chung, DC, Sahani, DV, Kalva, SP, Kozin, SV, Mino, M, Cohen, KS, Scadden, DT, Hartford, AC, Fischman, AJ, Clark, JW, Ryan, DP, Zhu, AX, Blaszkowsky, LS, Chen, HX, Shellito, PC, Lauwers, GY & Jain, RK (2004) *Nat Med* 10: 145-7.
16. Lammerts, E, Roswall, P, Sundberg, C, Gotwals, PJ, Koteliansky, VE, Reed, RK, Heldin, N-E & Rubin, K (2002) *Int J Cancer* 102: 453-62.
17. Salnikov, AV, Roswall, P, Sundberg, C, Gardner, H, Heldin, N-E & Rubin, K (2005) *Lab Invest* 85: 512-21.
18. Lee, CG, Heijn, M, di Tomaso, E, Griffon-Etienne, G, Ancukiewicz, M, Koike, C, Park, KR, Ferrara, N, Jain, RK, Suit, HD & Boucher, Y (2000) *Cancer Res* 60: 5565-70.
19. Salnikov, AV, Heldin, N-E, Stuhr, LB, Wiig, H, Gerber, H, Reed, RK & Rubin, K (2006) *Int J Cancer* 119: 2795-2802.
20. Ameye, L & Young, MF (2002) *Glycobiology* 12: 107R-16R.
21. Heinegard, D, Larsson, T, Sommarin, Y, Franzen, A, Paulsson, M & Hedbom, E (1986) *J Biol Chem* 261: 13866-72.
22. Svensson, L, Aszodi, A, Reinholt, FP, Fassler, R, Heinegard, D & Oldberg, A (1999) *J Biol Chem* 274: 9636-47.
23. Gill, MR, Oldberg, A & Reinholt, FP (2002) *Osteoarthritis Cartilage* 10: 751-7.
24. Jepsen, KJ, Wu, F, Peragallo, JH, Paul, J, Roberts, L, Ezura, Y, Oldberg, A, Birk, DE & Chakravarti, S (2002) *J Biol Chem* 277: 35532-40.
25. Ameye, L, Aria, D, Jepsen, K, Oldberg, A, Xu, T & Young, MF (2002) *Faseb J* 16: 673-80.
26. van 't Veer, LJ, Dai, H, van de Vijver, MJ, He, YD, Hart, AA, Mao, M, Peterse, HL, van der Kooy, K, Marton, MJ, Witteveen, AT, Schreiber, GJ, Kerkhoven, RM, Roberts, C, Linsley, PS, Bernards, R & Friend, SH (2002) *Nature* 415: 530-6.
27. Welsh, JB, Sapinoso, LM, Su, AI, Kern, SG, Wang-Rodriguez, J, Moskaluk, CA, Frierson, HF, Jr & Hampton, GM (2001) *Cancer Res* 61: 5974-8.

28. Garber, ME, Troyanskaya, OG, Schluens, K, Petersen, S, Thaesler, Z, Pacyna-Gengelbach, M, van de Rijn, M, Rosen, GD, Perou, CM, Whyte, RI, Altman, RB, Brown, PO, Botstein, D & Petersen, I (2001) *Proc Natl Acad Sci U S A* 98: 13784-9.
29. Murdoch, C, Muthana, M & Lewis, CE (2005) *J Immunol* 175: 6257-63.
30. Gordon, S (2003) *Nat Rev Immunol* 3: 23-35.
31. Kristjansen, PE, Boucher, Y & Jain, RK (1993) *Cancer Res* 53: 4764-6.
32. Ueno, H, Jones, AM, Wilkinson, KH, Jass, JR & Talbot, IC (2004) *Gut* 53: 581-6.
33. Sis, B, Sarioglu, S, Sokmen, S, Sakar, M, Kupelioglu, A & Fuzun, M (2005) *J Clin Pathol* 58: 32-8.
34. Hotary, KB, Allen, ED, Brooks, PC, Datta, NS, Long, MW & Weiss, SJ (2003) *Cell* 114: 33-45.
35. Geng, Y, McQuillan, D & Roughley, PJ (2006) *Matrix Biol* 25: 484-91.
36. Levick, JR (1987) *Q J Exp Physiol* 72: 409-37.
37. Znati, CA, Rosenstein, M, McKee, TD, Brown, E, Turner, D, Bloomer, W D, Watkins, S, Jain, RK & Boucher, Y (2003) *Clin Cancer Res* 9: 5508-13.
38. Brown, E, McKee, T, diTomaso, E, Pluen, A, Seed, B, Boucher, Y & Jain, RK (2003) *Nat Med* 9: 796-800.
39. Ohtani, O, Ushiki, T, Taguchi, T & Kikuta, A (1988) *Arch Histol Cytol* 51: 249-61.

FIGURE LEGENDS

Fig. 1. Expression of fibromodulin in carcinomas.

Immunoperoxidase staining of fibromodulin in PROb rat colonic carcinoma (A), DMBA induced rat breast carcinoma (B), mouse RIP-Tag insulinomas (C). Quantitative real time PCR of KAT-4 tumors from mice treated with conrol IgG_{2A} or Fc:TβRII (D). Staining of fibromodulin in control IgG_{2A}- (E) and Fc:TβRII- (F) treated mice carrying KAT-4 carcinomas. Fibromodulin staining of KAT-4 carcinoma xenografted in wild type (G) and fibromodulin-deficient (H) mice. Mice carrying KAT-4 carcinoma were treated with vehicle or Fc:TβRII (10 mg/kg) 10 days prior to sacrifice (16). Tumors were frozen, sectioned, stained with a rabbit anti-bovine fibromodulin antiserum and counterstained with hematoxylin (22) (Bar 100 μm).

Fig. 2. Tumor stroma ultrastructure.

Transmission electron micrographs of KAT-4 carcinomas grown in wild type (A), fibromodulin-deficient (B), control IgG_{2A}-treated (C) and Fc:TβRII-treated (D) mice (*x* 25,000, bar 200 nm). Morphometric analyses of collagen fibrils in carcinomas grown in wild type (open bars) and fibromodulin-deficient (filled bars) mice (E). Collagen fibril diameters in control IgG_{2A}- (open bars) and Fc:TβRII-treated (filled bars) carcinomas (F). Scanning electron micrographs of carcinomas grown in wild type (G) and fibromodulin-null (H) mice. Control IgG_{2A}- (I) and Fc:TβRII-treated (J) mice (*x* 300, bar 100 μm).

Fig. 3. Effect of fibromodulin deficiency on interstitial fluid pressure in carcinomas.

KAT-4 (A) or PROb (B) carcinomas were grown in wild type (wt), heterozygous (+/-) and fibromodulin-deficient (-/-) mice. IFPs were determined by the "wick-in-the-needle" technique as previously described (16).

Fig. 4. Analyses of vessel density, macrophage infiltration and regulation of fibromodulin mRNA by anti-inflammatory drugs in KAT-4 carcinomas.

KAT-4 carcinomas grown in wild type (open bars), fibromodulin heterozygous (stippled bars) and fibromodulin-deficient (filled bars) mice were subjected to immunohistochemistry to detect CD31-positive vessels (A), tumor infiltrating macrophages (B), and MHC class II-expression by macrophages (C). Athymic mice carrying KAT-4 carcinomas were treated with 30 mg/kg dexamethasone (n = 3) or rh-IL-1Ra (Kinaret^{R}; injected *s.c*. twice daily for 10 days with 7.5 mg; n = 2) (17). Fibromodulin mRNA levels were determined by real-time PCR using β-actin or GAPDH as an internal standards (D). mRNA levels are presented as percent of the levels in IgG_{2A}-treated control tumors (mean ± range).

TABLES

	EBD leakage (pixels per area unit) n=3	Dextran-perfused vessels (number per mm^2) n=3
Fmod +/+	74±5	43±10
Fmod -/-	70±3	45±3

Table I. Plasma protein leakage and dextran-perfused vessel density in KAT-4 tumors grown in fibromodulin-deficient mice. Plasma protein leakage from KAT-4 tumor blood vessels was determined by measuring the extent of EBD-labeled albumin extravasation. One area unit corresponds to 69 μm^2. FITC-dextran-perfused blood vessels were quantified under low magnification (*x* 200) according to Chalkley point-overlap morphometry.

	Extracellular volume (ECV) (ml/g dry weight) n=5		Plasma volume (ml/g dry weight) n=5		Total tissue water (ml/g dry weight) n=5	
	Tumor	Skin	Tumor	Skin	Tumor	Skin
Fmod +/+	1,78±0,42	1,91±0,69	0,13±0,12	0,06±0,05	5,27±0,20	2,69±0,42
Fmod -/-	2,59±0,63	1,88±0,68	0,11±0,06	0,04±0,02	5,77±0,67	2,62±1,23

Table II. Tumor extracellular fluid and plasma volumes. Extracellular fluid volumes in KAT-4 carcinomas were measured as extravascular distribution space of ^{51}Cr-EDTA after functional nephrectomy by the bilateral ligation of the renal pedicles via flank incisions. Plasma volumes were measured using ^{125}I-labeled human serum albumin (^{125}I-HSA; Institute for Energy Techniques, Kjeller, Norway). Both techniques have been detailed elsewhere (19).

Figure 1

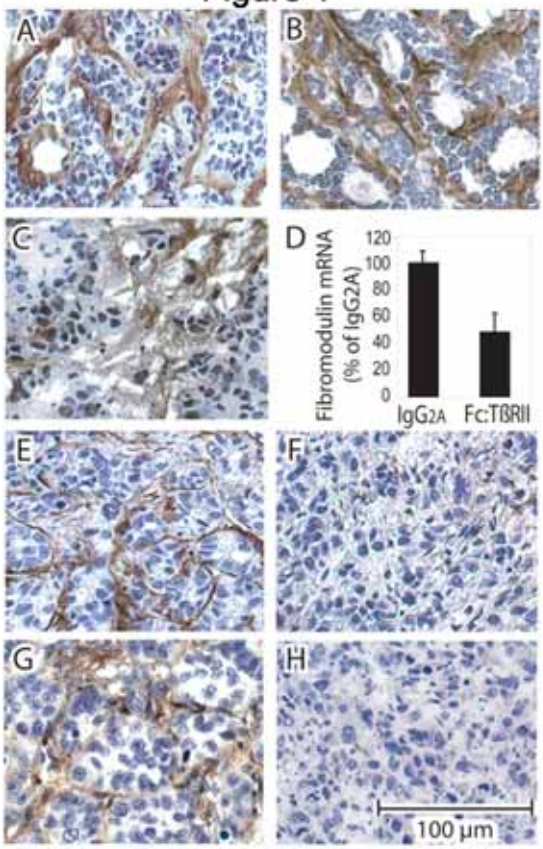

Figure 2

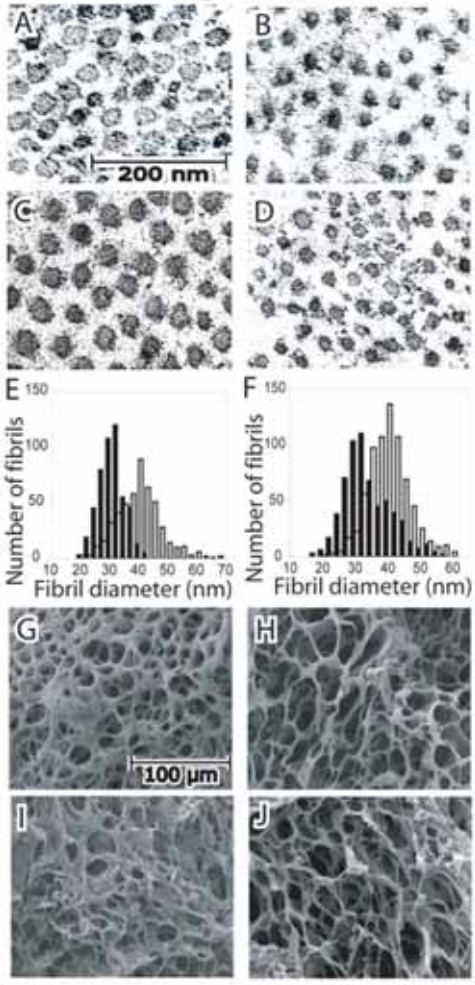

Figure 3

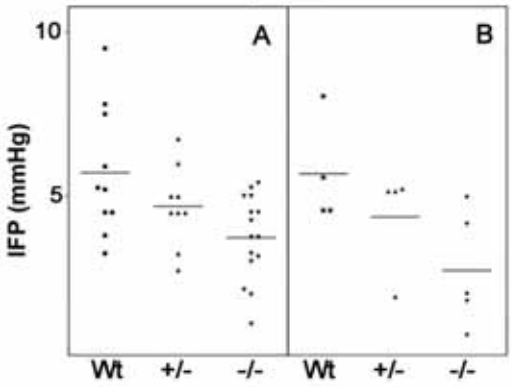

Figure 4